Title

Urocortin3 mediates somatostatin-dependent negative feedback control of insulin secretion

Journal

Nature Medicine, 21(7)

ISSN

1078-8956

Authors

van der Meulen, Talitha
Donaldson, Cynthia J
Cáceres, Elena
et al.

Publication Date

2015-07-01

DOI

10.1038/nm.3872

Peer reviewed

HHS Public Access

Author manuscript

Nat Med. Author manuscript; available in PMC 2016 January 01.

Published in final edited form as:

Nat Med. 2015 July ; 21(7): 769–776. doi:10.1038/nm.3872.

Urocortin3 mediates somatostatin-dependent negative feedback control of insulin secretion

Talitha van der Meulen[1,2], **Cynthia J. Donaldson**[2], **Elena Cáceres**[2], **Anna E. Hunter**[1,2], **Christopher Cowing–Zitron**[1], **Lynley D. Pound**[3], **Michael W. Adams**[4], **Andreas Zembrzycki**[5], **Kevin L. Grove**[3], and **Mark O. Huising**[1,2,6,*]

[1]Department of Neurobiology, Physiology & Behavior, College of Biological Sciences, University of California, Davis, CA, USA

[2]Clayton Foundation Laboratories for Peptide Biology, The Salk Institute for Biological Studies, La Jolla, CA, USA

[3]Division of Diabetes, Obesity and Metabolism, Oregon National Primate Research Center, Oregon Health and Science University, Beaverton, OR, USA

[4]Waitt Advanced Biophotonics Center, The Salk Institute for Biological Studies, La Jolla, CA, USA

[5]Molecular Neurobiology Laboratory, The Salk Institute for Biological Studies, La Jolla, CA, USA

[6]Department of Physiology & Membrane Biology, School of Medicine, University of California, Davis CA, USA

Abstract

The peptide hormone Urocortin3 (Ucn3) is abundantly expressed by mature beta cells, yet its physiological role is unknown. Here we demonstrate that Ucn3 is stored and co–released with insulin and potentiates glucose–stimulated somatostatin secretion via cognate receptor on delta cells. Further, we found that islets lacking endogenous Ucn3 demonstrate fewer delta cells, reduced somatostatin content, impaired somatostatin secretion and exaggerated insulin release, and that these defects are rectified by synthetic Ucn3 *in vitro*. Our observations indicate that the paracrine actions of Ucn3 activate a negative feedback loop that promotes somatostatin release to ensure the timely reduction of insulin secretion upon normalization of plasma glucose. Moreover, Ucn3 is markedly depleted from beta cells in mouse and macaque diabetes models and in human

*address all correspondence to mhuising@ucdavis.edu or 1–530–752–4670.

Accession codes

Sequencing data sets described in this work have been deposited in the Gene Expression Omnibus (GEO) repository under accession number GSE58286.

The authors have no conflicts to declare.

Author Contributions

T.v.d.M. and M.O.H. validated the mouse models generated over the course of this study and designed all mouse experiments. T.v.d.M., E.C., A.E.H., A.Z. and M.O.H. performed mouse experiments. T.v.d.M., C.J.D., A.E.H. and M.O.H. performed many islet isolations. C.J.D. performed all insulin and somatostatin hormone measurements and coordinated the receipt of human islets. E.C. and M.O.H. designed, performed and analyzed the continuous glucose monitoring experiment. C.C.–Z. and M.O.H. performed bioinformatics analysis. T.v.d.M. and M.O.H. conducted immunolabeling and acquired all images. M.W.A. performed Super Resolution Structured Illumination Microscopy and supported image acquisition and analysis. L.D.P. and K.L.G. designed and conducted the non–human primate studies and provided the histological material used in this study. M.O.H. conceived the study, was responsible for its overall design and planning and wrote the article together with T.v.d.M.

diabetic islets. This suggests that Ucn3 is a key contributor to stable glycemic control whose reduction during diabetes aggravates glycemic volatility and contributes to the pathophysiology of this disease.

Subject Terms

Biological sciences/Physiology/Metabolism/Homeostasis; Health sciences/Endocrinology; Health sciences/Diseases/Endocrine system and metabolic diseases/Diabetes/Type 2 diabetes; Biological sciences/Physiology/Metabolism/Metabolic diseases/Diabetes/Type 2 diabetes

Introduction

Insulin–secreting beta cells and glucagon–secreting alpha cells are organized in close proximity within the islets of Langerhans of the pancreas to facilitate the local coordination of the release of both hormones, which have diametrically opposing effects on the liver with respect to the regulation of hepatic glucose production[1–3]. Their response is critically dependent on ambient glucose as high glucose levels stimulate insulin secretion, while low glucose levels stimulate glucagon secretion as part of a counter–regulatory response to prevent hypoglycemia[4]. Somatostatin–secreting delta cells provide essential negative feedback to this process by inhibiting both insulin and glucagon release[5–9], thus ensuring that islet endocrine output is reset upon return of plasma glucose to its homeostatic setpoint. Type 2 and Type 1 diabetes are diseases of insufficient insulin signaling compounded by excess glucagon release[10], indicating dysregulation of the local mechanisms that balance insulin and glucagon release to ensure stable glycemic control over decades. Nevertheless, little is understood about the factors that promote somatostatin secretion to provide crucial negative feedback to beta and alpha cells[6]. Somatostatin release from delta cells is induced by glucose, sulfonylureas, amino acids, cholecystokinine and cyclic AMP and is inhibited by cholinergic stimulation[11–18], although these effects have invariably been demonstrated in pancreas or islet perfusion experiments that complicate the distinction between delta cell–autonomous actions and paracrine effects that involve non–delta cells.

Urocortin3 (Ucn3) is a peptide hormone that is exclusively expressed by beta cells in mouse islets, but is expressed by both beta and alpha cells in human[19–21]. It signals specifically via the type 2 corticotropin releasing hormone receptor (Crhr2)[22–24] and is a molecular marker of primary and embryonic stem cell–derived beta cell maturation[20,25,26]. Ucn3 is abundantly expressed by beta cells and was previously reported to promote insulin and glucagon release[19,27]. However, these studies also observed increased plasma glucose in response to Ucn3 administration[19] and increased glucose tolerance in Ucn3 null mice[27]; observations at odds with the reported insulinotropic actions of Ucn3, suggesting that its physiological role is poorly understood. We resolve this enigma by demonstrating that Ucn3 is co–secreted with insulin upon glucose–sensing and promotes somatostatin secretion from delta cells. As such, Ucn3 activates a negative feedback loop by amplifying somatostatin release to ensure that insulin and glucagon release are timely attenuated. The clinical significance of this negative feedback is illustrated by our observations that Ucn3 is depleted from beta cells in states of diabetes, coincident with the loss of stable glycemic control. We suggest that the

loss of Ucn3 reflects a breakdown in somatostatin–mediated negative feedback that contributes to the pathophysiology of diabetes.

Results

Ucn3 is a paracrine factor that targets delta cells

To delineate the physiological role of Ucn3, we compared the level of Ucn3 expression relative to that of other islet hormones. Ucn3 is abundantly expressed in islets (Supplementary Fig. 1) and ranks among the top–ten most abundantly expressed peptide hormones by islets and third–most by beta cells after insulin and islet amyloid polypeptide (Iapp) (Fig. 1a). Nevertheless, the abundance of *Ucn3* as measured by RNA–seq (Fig. 1a) and peptide content (Fig. 1b) in islets is several orders of magnitude lower than the expression of mouse *Ins1* and *Ins2* (Fig. 1a) and islet insulin content (Fig. 1b). *Ucn3* expression and content are also markedly lower than somatostatin (Fig. 1a, b), which acts locally within the pancreas. Moreover, glucose stimulates the co–release of Ucn3 with insulin from primary mouse islets *in vitro* (Fig. 1c), as previously shown for MIN6 insulinoma cells[27] and in line with their high degree of colocalization in secretory granules (Fig. 1d).

As Ucn3 is released at an approximately four orders of magnitude lower concentration than insulin and would quickly dilute further in the systemic circulation, it likely serves a paracrine role. We therefore sought to identify the islet cell type that expresses Crhr2 and responds to Ucn3 directly. We have previously demonstrated the presence of mRNA for the alpha isoform of *Crhr2* (*Crhr2α*) in mouse and human islets[28]. The lack of reliable antibodies combined with its relatively low abundance[28] have to date precluded the identification of the cell type(s) within the islet that express(es) Crhr2α and can respond to Ucn3. We therefore crossed a novel *mIns1*–H2b–mCherry reporter[21] to delta (*Sst*–Cre; Fig. 1e) or alpha (*Gcg*–Cre; Fig. 1f) cell reporter mice. Expression analysis by quantitative PCR on FACS–purified mCherry+ beta and YFP+ delta (Fig. 1g) and alpha (Fig. 1h) cells confirms that *Crhr2* is specifically expressed by delta cells (Fig. 1i). We also developed a novel *Crhr2α*–Cre transgenic reporter mouse, which confirmed lineage expression of *Crhr2α* in somatostatin–positive cells (Supplementary Fig. 2).

Endogenous Ucn3 promotes somatostatin secretion

We next turned to *Ucn3*–null mice[27], where transcriptome analysis confirmed the absence of *Ucn3* (Fig. 2a) and revealed marked reductions in the expression of known delta cell markers including *Sst*, *Rbp4*, and *Hhex*[29,30] compared to wild type littermates (Fig. 2b–d and Supplementary Table 1). These observations suggest that the absence of Ucn3 precipitated relative delta cell deficiency. Indeed, *Ucn3*–null islets displayed selective reductions in somatostatin content (Fig. 2e) and relative delta cell number (Fig. 2f) compared to controls. *Ucn3*–null islets demonstrate impaired basal and glucose–stimulated somatostatin release compared to wild–type islets, which we fully rescued by co–stimulation with synthetic Ucn3 (Fig. 2g). *Ucn3*–null islets hyper–secreted insulin during the first and second phase of secretion compared to controls, which normalized upon addition of synthetic Ucn3 peptide

(Fig. 2h, i). Islets from *Crhr2*–null mice[31] showed comparable defects in somatostatin content and release compared to wild–type littermate controls (Supplementary Fig. 3).

Next we tested the contribution of endogenous Ucn3 to somatostatin secretion. Ucn3 promoted the release of somatostatin under basal and high glucose (Fig. 3a). Co–stimulation with the Crhr2–selective antagonist Astressin2B (Ast2B)[32] prevented this. Notably, Ast2B by itself fully prevented somatostatin secretion induced by high–glucose conditions and returned somatostatin release to levels no different from those observed under basal–glucose *in vitro* (Fig. 3a).

We determined that glucose–stimulated somatostatin secretion is inhibited by the ATP–sensitive potassium channel (K_{ATP}) agonist diazoxide and by the L–type calcium channel blocker isradipine, as is well established for insulin secretion[33] (Fig. 3b). We then tested if glucose acts primarily on beta cells to induce the release of Ucn3 (Fig. 1c), which then triggers somatostatin release, or if Ucn3 amplifies somatostatin release triggered by delta cell–autonomous glucose sensing. Co–stimulation with Ucn3 under high–glucose conditions potentiates somatostatin release and inhibits insulin secretion (Fig. 3b). Similarly, Ucn3 potentiates the somatostatin release triggered by sulfonylureas (Fig. 3c). However, exogenous Ucn3 cannot overcome the inhibition of somatostatin secretion imposed by either diazoxide or isradipine (Fig. 3b).

We further explored the contribution of endogenous Ucn3 to insulin output in perfusion experiments. Acute inhibition of endogenous Ucn3 by Ast2B during the second phase of insulin secretion caused an immediate elevation in insulin secretion compared to control (Fig. 3d) secondary to alleviated Ucn3–dependent, somatostatin tone (Fig. 3e). Furthermore, Ast2B enhanced the potentiation of glucose–stimulated insulin secretion induced by a sub–maximal dose of exendin4 (Fig. 3g).

We next assessed the contributions of Ucn3–mediated somatostatin repression on glucose homeostasis *in vivo*. Pre–treatment with Ucn3 caused a marked delay in glucose clearance (Fig. 3g), accompanied by lower plasma insulin 10 minutes after glucose challenge (Fig. 3h) compared to saline controls, in agreement with Ucn3–stimulated somatostatin repressing insulin as demonstrated *in vitro* (Fig. 3a–e). Somatostatin antagonists fully prevented the robust reduction in glucose tolerance caused by acute Ucn3 administration (Fig. 3i).

Mindful of the conspicuous differences between rodent islets, where Ucn3 is exclusively expressed in beta cells, and primate islets, where Ucn3 is expressed by both beta and alpha cells[20,25], we measured the ability of Ucn3 to promote somatostatin release from human islets. Ucn3 stimulated somatostatin release from human islets under both basal and hyperglycemic conditions (Fig. 3j). Ast2B blocked the actions of Ucn3 and tended to inhibit glucose–stimulated somatostatin secretion from human islets (Fig. 3j), similar to our observations in mouse islets (Fig. 3a). Under hypoglycemic conditions associated with alpha cell activity, Ast2B inhibited somatostatin secretion (Fig. 3j).

Loss of Ucn3 expression is a hallmark of diabetes

Ucn3 expression appears relatively late during pancreas development and coincides with the acquisition of functional maturity by human embryonic stem cell–derived beta cells, suggesting that Ucn3 is a hallmark of maturity[20,25,26]. We therefore assessed Ucn3 expression during diabetic conditions associated with beta cell dysfunction. Ucn3 content and message are markedly lower in beta cells from leptin–deficient (*ob/ob*) mice (Fig. 4a, b) and leptin receptor–deficient (*db/db*) mice (Fig. 4c) compared to lean age–matched controls. This is not the result of congenital deficiencies in leptin signaling, as Ucn3 in *ob/ob* islets is not lower compared to lean littermates until the onset of obesity and frank diabetes around four weeks of age (Supplementary Fig. 4). Glucose–stimulated somatostatin release from *ob/ob* islets is impaired in comparison to lean controls and no longer inhibited by Ast2B (Fig. 4d), which is in line with the loss of endogenous Ucn3. We hypothesized that the resulting loss of negative feedback would cause increasingly volatile plasma glucose levels and adapted a method for continuous glucose monitoring for use in mice to assess this (Fig. 4e and Supplementary Video 1). Continuous measurement of glucose at 5–minute intervals over 72 hours in freely moving, untethered animals in their home cage illustrates the great accuracy of plasma glucose control in lean control mice (Fig. 4e). In sharp contrast, plasma glucose profiles of diabetic *ob/ob* littermates acquired simultaneously (Fig. 4e) not only visualized the robustly elevated average plasma glucose values that define diabetes, but reveal lengthened period and increased variance compared to lean controls (Supplementary Table 2).

To specifically interrogate the role of islet Ucn3 in glucose homeostasis, we generated a novel transgenic mouse model that over–expresses Ucn3 selectively in beta cells upon doxycycline administration, contingent on the presence of two distinct transgenes (Supplementary Fig. 5) and crossed this onto the *ob/ob* background. We induced transgenic Ucn3 in bitransgenic *ob/ob* mice at 6.5 weeks, when moderate diabetes and obesity had set in and when endogenous Ucn3 had disappeared (Fig. 4f and Supplementary Fig. 4). Restoration of Ucn3 in *ob/ob* mice acutely elevated plasma glucose levels compared to pre–induction and they remained higher than non–inducible *ob/ob* controls for the remainder of the experiment, independent of body weight (Fig. 4g). Induction of transgenic Ucn3 in lean mice, which maintain endogenous Ucn3, had no effect (Fig. 4g). Induction of transgenic Ucn3 similarly led to an exacerbation of hyperglycemia in mice rendered diabetic by the beta–cell toxin streptozotocin (STZ), which markedly reduces beta cell mass and depleted residual beta cells of Ucn3 (Supplementary Fig. 6). In a third experiment, we built on previous observations that established that full expression of endogenous Ucn3 does not occur until 2 weeks post–partum[20] and coincides with the elevation in glucose and drop in insulin that occur around this age[26,34]. Administration of doxycycline to pregnant dams unable to express transgenic Ucn3 themselves from embryonic day (E)10.5 onwards resulted in the premature expression of Ucn3 in bitransgenic offspring (Fig. 4h), causing premature elevations in plasma glucose at post–natal day (P)2 and P10 compared to control littermates (Fig. 4i). Onwards from three weeks post–parturition, when endogenous Ucn3 is fully expressed (Fig. 4j), transgenic Ucn3 no longer affected plasma glucose (Fig. 4i) as previously observed in non–diabetic bitransgenic controls (Fig. 4g and Supplementary Fig. 6).

Loss of Ucn3 in beta cells from diabetic humans and macaques

Shortly after birth, human UCN3 is present in both alpha and beta cells[20,25], a pattern that persisted in islets from lean, non–diabetic donors (Fig. 5a and Supplementary Fig. 7a). In contrast, islets from Type 2 diabetic donors across a range of body mass indices (BMIs), demonstrated selective depletion of UCN3 levels from beta cells, while alpha cells retained UCN3 expression (Fig. 5b and Supplementary Fig. 7b).

To further corroborate that UCN3 in beta cells is preferentially down–regulated compared to alpha cells upon metabolic challenge, we assessed UCN3 staining in a cohort of macaques chronically maintained on a high–fat diet, stratified into 'diet–resistant' and 'diet–sensitive' cohorts[35] (Supplementary Table 3). Islets from control macaques on normal diet demonstrated intense UCN3 immunoreactivity in both beta and alpha cells (Fig. 5c). In contrast, islets from macaques on the high–fat diet display selectively reduced UCN3 immunoreactivity in beta cells, which was particularly apparent in the diet–sensitive, insulin–resistant cohort (Fig. 5d, e and Supplementary Fig. 8).

Discussion

Here, we demonstrate that Ucn3 constitutes a local signal that under hyperglycemic circumstances promotes a negative feedback loop that attenuates insulin release via somatostatin (Fig. 6a). Previously, Ucn3 was proposed to engage in autocrine feedback to promote insulin release[19,27], but the discovery here that Crhr2 is absent on primary beta cells and is expressed by delta cells makes this model untenable. Moreover, our observations of increased plasma glucose upon Ucn3 administration[19], decreased glucose tolerance following Ucn3 administration that depends on uninterrupted feedback by endogenous somatostatin and increased glucose tolerance following *Ucn3* deletion[27] are difficult to reconcile with an insulinotropic role for Ucn3. Instead, these observations are fully compatible with the key role of Ucn3 in somatostatin–mediated negative feedback that we propose here. Furthermore, the de–repressed insulin release that acutely normalizes upon application of exogenous peptide phenocopies the hyperinsulinemia associated with islets null for *Sst*[16] or the delta cell–specific transcription factor *Hhex*[29], which offers strong support for the participation of Ucn3 and somatostatin in the same negative feedback loop. Reduced delta cell number and somatostatin content may contribute to impaired glucose–stimulated somatostatin release in *Ucn3*–null mice compared to controls. Nevertheless, inhibition of endogenous Ucn3 with Ast2B acutely affects somatostatin and thereby insulin secretion, establishing that endogenous Ucn3 participates in the physiological control of somatostatin release. Mechanistically, the co–dependence of somatostatin secretion on the class B GPCR ligand Ucn3 and delta cell–autonomous stimulus–secretion coupling mediated by K_{ATP} and L–type calcium channels, resembles the well–known glucose–dependent, insulinotropic actions of incretins on beta cells (Fig. 6b, c). Blocking the actions of endogenous Ucn3 and somatostatin with Ast2B is additive to the potentiating effects of incretins on glucose–stimulated insulin secretion, offering further support for the notion that Ast2B and incretins increase insulin secretion by distinct mechanisms.

Clustering of alpha, beta and delta cells enables crosstalk, either via the islet microcirculation or through communication by an assortment of paracrine signals[36–39]. It is

debated whether the circulation in the rodent islet favors mantle–to–core communication[40–42] or *vice versa*[43–45]. The Ucn3–dependent, somatostatin–mediated negative feedback loop that we discovered depends on both. Several factors can resolve the discrepancy between the suggested unidirectionality of the communication between the different cell types of the islets that is based on classical anatomical studies and the reality of bi–directionality crosstalk we demonstrate here. First, recent work[46] elegantly visualizes prior suggestions[40,41] of dynamically regulated local blood flow within the islet microcirculation that can locally reroute blood flow. Second, delta cells have well–developed projections that receive and release paracrine signals at some distance from the cell body[8]. Third, beta cells are well–connected through gap–junctions that synchronize insulin release across all beta cells in an islet[47–49], suggesting that it may not be necessary for each individual beta cell to receive direct somatostatin–mediated feedback to ensure effective inhibition of the entire pool. Of course the architecture of adult human islets features a much greater degree of intermingling of alpha and delta with beta cells, facilitating the multi–directional crosstalk we discovered (Fig. 6).

The late onset of Ucn3 expression in development[20,25,26] agrees with its role as the major paracrine signal to promote somatostatin–mediated feedback; until E15.5 when delta cells appear in substantial numbers[50,51], such a signal would serve no purpose. The importance of Ucn3–dependent negative feedback is evident under diabetic conditions, where the loss of Ucn3 not only correlates with hyperglycemia, but is associated with increased glycemic volatility. Paradoxically, restoration of Ucn3 by beta cells in several paradigms of relative beta–cell insufficiency aggravated hyperglycemia, consistent with Ucn3 imposing negative feedback on insulin release. This also explains why *Ucn3*–null mice maintain glucose tolerance following high–fat diet feeding[27]. Perhaps the down–regulation of UCN3 in beta cells of diabetic subjects is not a passive response to the adverse consequences of gluco– and lipotoxicity, but instead reflects an innate ability by the beta cell to actively adapt to changes in glucose demand by releasing the brake on insulin release. However, as paracrine actions of beta cell–derived factors inhibit alpha cell activity under normal circumstances[6,52,53], down regulation of UCN3 in beta cells of diabetic individuals may also disrupt somatostatin–mediated negative feedback on alpha cells. The therapeutic potential for this UCN3–mediated feedback loop is determined by its net effect on the combined inhibition of insulin and glucagon. Restoring Ucn3 in a setting of relative insulin deficiency, such as obesity or STZ–mediated partial beta cell ablation, may aggravate diabetes by repressing residual beta cell function, as shown here. However, in established Type 1 diabetes without meaningful residual beta cell function, Ucn3 could re–engage somatostatin–mediated negative feedback on alpha cells and curb the hyper–glucagonemia that aggravates diabetes[10,53].

In conclusion, we demonstrate that Ucn3 is stored in the insulin granules and is released along with insulin upon glucose stimulation. This released Ucn3 then engages a negative feedback loop by promoting the release of somatostatin from delta cells to inhibit further insulin secretion. We also found that inhibition of Ucn3 impairs glucose–stimulated somatostatin secretion and de–represses insulin release, indicating that Ucn3 is the major beta cell–derived factor to potentiate somatostatin release. Given the ingenious ways in

which healthy islets maintain tight glycemic control over a lifetime, such new insight may allow the development of novel therapies that rebalance insulin and glucagon release to better manage diabetes care.

Online Methods

General experimental approaches

No samples, mice or data points were excluded from the reported analysis with the following two exceptions. 1) For the STZ experiment, we excluded STZ–treated animals that failed to develop hyperglycemia (defined as plasma glucose >200 mg/dl; 1 wild type and 2 bitransgenic animals) at the start of induction at 6 weeks. 2) For hormone secretion experiments, on rare occasions, individual samples yielded very high values in both technical replicates that we attributed to the carry–over of an islet during supernatant collection. Such samples were excluded from the analysis as were samples with hormone concentrations below the minimum detectable dose. Insofar as distribution of animals across experimental groups was not determined by their genotype, we randomized to experimental groups unless noted otherwise. For glucose tolerance tests we organized treatments in random order and assigned animals by picking animals at random from their home cages in the morning of the experiment. To avoid bias in islet hormone secretion experiments (static and perfusion), we hand–picked the required number of islets per well/chamber from a pool of all islets and assigned each batch as the next replicate to each subsequent treatment. Experiments were performed in a blinded fashion as noted below. Animal experiments were generally monitored by an investigator with no in–depth knowledge of the expected outcome. During glucose tolerance tests (GTTs), an assistant recorded glucose values and evaluated these only after the conclusion of the test. During the continuous glucose monitoring experiment, receivers were blinded and did not display any glucose data to the investigator performing calibration measurements. The measurements of plasma glucose in the premature Ucn3 induction experiment at P2 and P10 was done on full litters before their genotypes were determined. All hormone concentrations were measured in duplicate by a different investigator from the one carrying out the secretion assay, who had no in–depth knowledge on the expected outcome of an experiment.

Biological materials and ethics statements

All *in vivo* experiments were carried out on male mice, with the exception of the induction of Ucn3 on an *ob/ob* background, which we conducted on females as our crosses did not yield Ucn3–inducible *ob/ob* males at the anticipated 1:32 ratio. We obtained commercial male C57BL/6NHsd mice from Harlan (Indianapolis, IN) at 6 weeks of age, which were used between 8 and 16 weeks of age. We maintained mice in group–housing on a 12–h light/12–h dark cycle with free access to water and standard rodent chow. We isolated islets as previously described[54]. Mice null for *Ucn3* (*Ucn3*^{tm1Pbl}) or *Crhr2* (*Crhr2*^{tm1Kflee}) have previously been described[27,31]. We monitored blood glucose levels by glucose stick from the tail (One–touch Ultra2, LifeScan, Chesterbrook, PA) except for early postnatal measurements, which were terminal. We obtained approval for all mouse procedures from the Salk Institute for Biological Studies Institutional Animal Care and Use Committee and performed experiments in compliance with the Animal Welfare Act and the ILAR Guide to

the Care and Use of Laboratory Animals. We obtained human islets via the NIDDK–supported Integrated Islet Distribution Program (IIDP). We obtained human donor pancreata from 18 donors (11 female, 7 male), ranging in age from newborn to 72 years via the Network of Pancreatic Islet Donors with Diabetes (nPOD). The Salk Institute for Biological Studies Institutional Review Board declared the human islet material and the human pancreas histological specimens used in this study exempt from IRB review under 45 CFR 46.101 (b) Category (4) on April 16, 2008 and August 6, 2013, respectively. We obtained macaque pancreas samples from the Oregon National Primate Research Center (ONPRC) Obese Resource, from 17 male rhesus macaques (*Macaca mulatta*) (15 adults from 6.5 to 14 years of age, and two one–year old juveniles) that were euthanized for other studies and are described in detail elsewhere[35]. Briefly, control animals were maintained on a 14.6% fat calories diet (Test Diet, Richmond, IN, USA), high–fat diet animals were maintained on a 36% fat calories diet, supplemented with 500 ml of Kool–Aid + 20% fructose three times a week. Food intake was recorded daily, water was provided *ad libitum* and lights were on from 7 am to 7 pm. Macaque care and procedures were done according to the ONPRC Institutional Animal Care and Use Committee at the Oregon Health and Science University. Cell lines used (HEK293T and Ins1[57]) were not formally authenticated, but displayed characteristics consistent with their phenotype, including the expression of insulin and secretion of Ucn3 for Ins1 cells. We did not screen for mycoplasma infection.

Generation of transgenic mice

We generated inducible Ucn3 transgenic mice by inserting the full mouse *Ucn3* coding region downstream of a doxycycline inducible promoter consisting of seven tetO–responsive elements followed by a minimal CMV promoter. We inserted the full mouse Ucn3 coding region downstream of a doxycycline–inducible promoter (Supplementary Fig. 5a). To validate that the expression of Ucn3 from the transgenic cassette is doxycycline–dependent and yields processed, bioactive Ucn3 peptide, we transiently transfected the cassette into Ins1 rat insulinoma cells[57] along with a helper vector encoding reverse tetracycline transactivator protein. Conditioned media from Ins1 cells stimulated with doxycycline dose–dependently stimulated Crhr2, as measured by cAMP response element–dependent luciferase activity in HEK293T cells[56] (Supplementary Fig. 5b). Conditioned media from non–induced Ins1 cells has residual activity on Crhr2, likely attributable to endogenous rat Ucn3 that is secreted by Ins1 cells. Application of the same conditioned media to cells carrying Crhr1 did not induce luciferase activity (Supplementary Fig. 5c), demonstrating that transgenic Ucn3 produced by Ins1 cells upon doxycycline stimulation is processed into a bioactive form that recapitulates the strict receptor preference of synthetic Ucn3 for Crhr2. Conditioned media from HEK293T cells transiently transfected with the pTREtight–mUcn3 construct and the appropriate helper vector and stimulated with doxycycline did not promote Crhr2–dependent luciferase production, indicating that post–translational processing by the beta cell is required for the production of bioactive Ucn3 (not shown). We linearized this construct and used it to generate a transgenic mouse line. We obtained five founder lines, of which one founder did not pass on the transgene to its offspring. We crossed the remaining four founder lines to *rip*–rtTA mice to generate doxycycline–inducible, beta cell–specific over expression of Ucn3. We evaluated each and maintained the line that combined the highest levels of transgenic mUcn3 message with no detectable ectopic expression at non–

pancreatic sites. In brief, using primers that distinguish between endogenous and transgenic Ucn3 transcripts and a third primer set that detects total *Ucn3* message levels (Supplementary Fig. 5a), we detected robust induction of transgenic *Ucn3 in vivo*, effectively doubling total *Ucn3* message levels, but only in islets of an animal that carries both the pTREtight–mUcn3 and *rip*–rtTA transgenes and received doxycycline (Supplementary Fig. 5d). Backcrossing of pTretight–mUcn3 x *rip*–rtTA bitransgenic animals on a *Ucn3* null background (Supplementary Fig. 5e) reveals that the doxycycline–mediated induction of Ucn3 is mosaic and restricted to a relatively small subset of beta cells (Supplementary Fig. 5f). Bitransgenic animals, when naive to doxycycline, show normal intra–peritoneal glucose tolerance (Supplementary Fig. 5g), but after one week of doxycycline exposure develop notable glucose intolerance in line with a mechanism of Ucn3–induced somatostatin–mediated repression of insulin release (Supplementary Fig. 5h). Comparison of the susceptibility of *rip*–rtTA and pTREtight–mUcn3 single transgenic animals to the diabetogenic effects of STZ reveals that *rip*–rtTA single transgenic animals are innately protected from STZ–induced diabetes, while pTREtight–mUcn3 transgenic animals are not (Supplementary Fig. 5i) This suggests that the partial protection against STZ–mediated hyperglycemia we observed in bitransgenic animals (Supplementary Fig. 5i) is likely attributable to the presence of the *rip*–rtTA transgenic cassette. We administered doxycycline by custom diet (Harlan Teklad, Madison, WI) at 1000 mg/kg.

The generation of the *mIns1*–H2b–mCherry reporter mouse that faithfully and selectively marks all beta cells by nuclear expression of a histone2B–mCherry fusion protein under control of the 10 kb mouse *Ins1* promoter is described in detail elsewhere[21]. Crossed to either *Sst*–Cre[58] or *Gcg*–Cre[59] and *Rosa*–lsl–YFP[60] transgenic lines these mice facilitate FACS–mediated collection of highly pure beta, delta and alpha cells from dissociated mouse islets. Each sample consists of a pool of dissociated islets from a dozen triple transgenic animals hemizygous for each transgene.

To generate *Crhr2α*–mCherry–Cre reporter mice, we manipulated a 140 kb BAC clone (RP24–351G5; bacpac.chori.org) by homologous recombination to replace the start codon of the alpha isoform of the Crhr2 gene in exon 3, which is skipped in the beta isoform of Crhr2, with a reporter cassette containing mCherry fused to Cre recombinase by a constitutively proteolytic f2A processing site. We used a neomycin selection marker flanked by FRT sites for positive selection, which we later removed by crossing our founder to an actin–FLP1 mouse. We never detected mCherry protein expression and attribute this to the relatively low quantum yields of mCherry coupled to the fact that the promoter for *Crhr2α*, like many receptor promoters, is relatively weak. We generated all three mouse lines by pro–nuclear injection in CB6F1 hybrids (C57BL/6 males x Balb/c females, The Jackson Laboratory, Sacramento, CA; stock #100007) by the Salk transgenic core under supervision of Ms. Yelena Dayn, and backcrossed to the C57bl6 background.

Glucose tolerance test and insulin release

We weighed animals in the morning after an overnight fast (Supplementary Table 4). For a GTT or insulin release, male mice received a single 2 g/kg i.p. injection of glucose (dextrose; Sigma, St. Louis, MO, D9559) at time = 0. We determined plasma glucose levels

using tail vein blood by glucometer (OneTouch Ultra2; LifeScan, Milpitas, CA). We collected blood by retro–orbital bleed to determine plasma insulin levels using an RIA kit (EMD Millipore, Billerica, MA; catalog; #SRI–13k). Where indicated, we pretreated male mice at t = −5 min. with mouse Ucn3 peptide, the Crhr2 antagonist Astressin2B[32] or an equimolar mixture of the somatostatin receptor antagonists Sst3–ODN–8 (Carbamoyl–des–AA^{1,2,4,5,12,13}[D–Cys3, Tyr^{7}, D–AgI^{8} (Me,2–napthoyl)]–SS; #315–260–15)[61] and Sst2 ant. (H_2N–*p*NO_2Phe^{2}–[DCys^{3}–Tyr^{7}–DAph(Cbm)^{8}–Lys^{9}–Thr^{10}–Cys^{14}]–2Nal^{15}–NH_2; #406–028–15)[62], all at 100 nmol/kg i.p. in saline. All peptides were synthesized in–house using a *tert*–butyl–oxy–carbonyl strategy, characterized by mass spectrometry and purified to >98% purity by reverse phase high pressure liquid chromatography.

Continuous glucose measurements

We anaesthetized mice by an i.p. injection of a cocktail of ketamine (80 mg/kg) and xylazine (8 mg/kg)) and shaved and sterilized the flat of their back. We gently introduced Dexcom Seven–plus continuous glucose sensors (Dexcom Inc., San Diego, CA) subcutaneously in two *ob/ob* males and two lean age–matched males at 10 weeks of age by means of a modified technique with a guiding needle for sensor insertion. We attached and affixed the transmitters to the back of the animal using acrylamide–based veterinary glue. We started and calibrated the sensors per instructions before the beginning of the dark cycle using glucose values obtained by hand–held glucometer from the tip of the tail. We carried out calibration measurements twice daily, at the beginning and the end of the light cycle. We collected continuous glucose profiles for up to seven days in freely moving animals in their home cage (Supplementary Video 1, Fig. 4e). We did not use glucose data acquired prior to calibration on the morning after implantation as the hyperglycemia associated with anesthesia affected the glucose profile. We recovered transmitters under isoflurane anesthesia or following euthanasia. We acquired body composition measurements by an EchoMRI–100H body composition analyzer (Echo Medical Systems, Houston, Tx), according to the manufacturer's instructions.

STZ treatment

We induced stable hyperglycemia in males by treatment on 5 consecutive days with the beta cell toxin STZ (Calbiochem; now EMD Millipore, Billerica, MA) dissolved fresh in 100 mM sodium citrate (pH 4.5) immediately before administration by i.p. injection. We injected wild type mice with 50 mg/kg daily, while bitransgenic mice received 70 mg/kg daily to compensate for the reduced diabetogenic actions of STZ in mice that carry the rtTA transgene (Supplementary Fig. 5i). We excluded STZ–treated animals that failed to develop hyperglycemia (defined as plasma glucose >200 mg/dl; 1 wild type and 2 bitransgenic animals) at the start of induction at 6 weeks. We ranked STZ–treated bitransgenic animals at this time based on their average plasma glucose values over the preceding 3 weeks and alternatingly assigned them to the doxycycline–induced and chow control groups.

Deep sequencing

We isolated RNA from Trizol by a chloroform extraction, assisted by phase lock tubes (5 Prime, Gaithersburg, MD). We precipitated RNA by isopropanol and cleaned up over an

RNEasy microcolumn (Qiagen, Valencia, CA) per the manufacturer's instructions, taking great care to avoid carry over of ethanol following the column washes. Following elution in 30 microliter elution buffer, we verified RNA quality by BioAnalyzer (Agilent, Santa Clara, CA). We generated Indexed sequencing libraries using the TruSeq RNA sample Prep Kit v2 (Illumina Inc. San Diego, CA) and sequenced at 50 cycles, single read on an Illumina HiSeq 2000 platform. We mapped sequencing reads from *Ucn3* null and wild type islets (n = 3 individuals each) to mouse genome version mm9 (NCBI build 37) using STAR[63]. We sequenced at least 42 million reads for each library. We used bedtools[64] to create count tables of the sorted bam files using reads aligning to RefSeq defined exons and used DESeq[65] for statistical comparison. We prepared normalized genome browser tracks using HOMER (http://homer.salk.edu)[66] and uploaded into the University of California Santa Cruz genome browser to generate browser plots.

qPCR

We determined gene expression from cDNA of FACS–purified delta, beta and alpha cells and normalized to *Hprt* as previously described[28] on a Lightcycler 480 (Roche, Indianapolis, IN) using validated primers designed using the online universalprobelibrary.com design feature and listed in Supplementary Table 5.

Peptide hormone assays

We isolated islets for secretion experiments by injecting collagenase up the ductal tree through the common bile duct and cultured overnight in RPMI (11 mM glucose, 10% fetal bovine serum, pen/strep) as previously described[54]. We conducted all secretion experiments in Krebs Ringer Buffer. To avoid bias in static secretion experiments, we hand–picked the required number of islets per well from a pool of all islets and assigned as the next replicate to each subsequent treatment. We carried out islet perfusions using a custom–built perfusion setup with six parallel chambers. We measured human and mouse insulin and glucagon secretion and peptide content with commercially available RIA kits (EMD Millipore, Billerica, MA; catalog numbers #HI–14k, #SRI–13k and #GL–32k) per the manufacturer's instructions. We measured somatostatin by the same RIA that was developed in–house following the discovery of somatostatin[67] using an anti–Sst–14 antiserum developed in–house (S201; diluted 1:50,000)[68]. We previously described general RIA buffers and procedures[69]. We radiolabeled Tyr^0–Sst14 with ^{125}I by the chloramine T oxidation method and a 1:1:10 molar ratio of peptide:$Na^{125}I$:chloramine T. We purified tracer by HPLC using a 0.1% trifluoroacetic acid–acetonitrile solvent system and a diphenyl column. We used synthetic Sst–14 as standard, EC_{50} and minimal detectable dose are 12 pg/tube and 1 pg/tube, respectively. We measured Ucn3 by an RIA we developed in–house using an anti–mUcn3 antiserum (#7255; diluted 1:300,000) from approximately 1000 pooled islets in a 100 µl volume over the course of 4 hours. We iodinated Tyr^0Nle^{12}–mUcn3 as above for use as a tracer and used synthetic mUcn3 as a standard. EC_{50} and minimal detectable dose are 20 pg/tube and 1 pg/tube, respectively. Cross–reactivity to rUcn1 and r/hCRH was < 0.01% and to mUcn2 <0.5% and no message for *Crh*, *Ucn1* and *Ucn2* can be detected in mouse islets[21].

Immunohistochemistry

We conducted immunohistochemistry as previously described[20] using primary antibodies against Ucn3 (rabbit anti–human Ucn3; generated in–house; #7218, 1:2000), insulin (guinea pig anti–insulin; Dako Cytomation Inc, Carpinteria, CA; #A0564, 1:500) or (mouse anti–insulin; Abcam, Cambridge, MA; #ab6995, 1:1000), glucagon (guinea pig anti–glucagon; EMD Millipore, Billerica, MA; #4031–01F, 1:7000), somatostatin (sheep anti–somatostatin; American Research Products Inc., Waltham, MA; #13–2366; 1:1000), or LacZ (chicken anti–LacZ; Abcam, Cambridge, MA; #ab9361, 1:1000). We colocalized insulin and Ucn3 in mouse beta cells at sub–cellular resolution on 2 micron thick paraffin slides of mouse pancreas by Super Resolution Structured Illumination Microscopy (SR–SIM) using a Zeiss Elyra PS.1 Super Resolution Microscope. We used an automated iterative maximum correlation threshold (MCT) algorithm[70] to determine thresholds for the insulin and Ucn3 signal before the determination of the thresholded Manders' coefficients for insulin with Ucn3 and Ucn3 with insulin. We generated the colocalization pixel map in Imaris. We applied masks to human islet images using the same MCT method based on insulin and glucagon staining to isolate and compare Ucn3 intensity in beta and alpha cells of the same human islet. All confocal images were acquired at 63x using a 1.4NA oil immersion lens at 1024 × 1024 resolution (pixel dimension 0.22 × 0.22 μm) applying 2x line average and acquiring each channel sequentially. We acquired images at the Waitt Advanced Biophotonics Center Core Facility at the Salk Institute and at the Veterinary Medicine Advanced Imaging Facility and Plant Biology core facilities at UC Davis.

Statistics

We conducted statistics in Prism 6.0e for Mac (Prism, GraphPad Software, Inc.). We reported all values as mean values across biological replicates and assumed normality, unless otherwise noted. We evaluated experiments with more than two treatments by ANOVA, followed by Student's t–test to determine which means differed statistically, applying Welch's correction for unequal variance when necessary. Experiments with multiple treatments across genotypes were evaluated by two–way ANOVA, followed by Holm–Sidak's multiple comparison test. We evaluated perfusion data by two–way ANOVA for treatment and the interaction of treatment and time for each block. We assessed the effects of *in vivo* Ucn3 induction on plasma glucose by linear regression for differences in slope and intercept between groups before and after induction. We tested all data two–tailed, with exception of the perfusion data, the human islet somatostatin secretion data and the Ucn3 induction data, which we evaluated one–tailed under the hypothesis, formulated by prior mouse static secretion experiments, that Ucn3 stimulates somatostatin release. We evaluated differences in deep sequencing data by DESeq. We evaluated variation in continuous glucose monitoring by the Brown–Forsythe test for the equality of variances based on median glucose values as summarized in Supplementary Table 2. We subsequently evaluated differences in mean glucose values and period length by Student's t–test with adjustment for unequal variances. We based the desired minimal number of animals per group (n) for GTTs on prior experience in comparable experiments[54] and on common practice in the field for these experiments and adopted an n that sufficed to detect a 50% change in the mean (assuming a standard deviation of 40%, a significance level p of 0.05,

and a power of 0.8). The number of replicates per group for experiments on Ucn3–inducible animals was limited by the number of experimental animals we could reasonably generate (for example, only 1 in 16 offspring of either sex of the cross to generate Ucn3–inducible *ob/ob* animals carried the required combination of transgenes and alleles). Continuous glucose monitoring was limited to 4 animals by the number of available sensors. We based the number of replicates in static secretion experiments on prior experience with these assays although the total number of islets required per well typically limited the number of replicates in somatostatin and Ucn3 secretion assays. The number of replicates in islet perfusion experiments was limited to the number of parallel slots available in the fraction collector.

Supplementary Material

Refer to Web version on PubMed Central for supplementary material.

Acknowledgments

We dedicate this work to the memory of Dr. Wylie W. Vale, who co–discovered both somatostatin (in 1973) and Urocortin 3 (in 2001) and who would have been delighted in their participation in the same feedback loop. We acquired images at the Waitt Advanced Biophotonics Center at the Salk Institute and at the Veterinary Medicine Advanced Imaging Facility and Plant Biology core facilities at UC Davis. N. Justice (University of Texas Health Science Center at Houston) is acknowledged for generating the BAC construct used to generate the Crhr2α–mCherry–Cre reporter line. J. Vaughan is acknowledged for iodination of tracers and H. Park, K. Tigyi and S. Dólleman for their excellent assistance with various aspects of these studies. R. Yang and K. Nakamura at Dexcom Inc. are acknowledged for their assistance in unblinding CGM data at the conclusion of the CGM experiment. We performed this research with the support of the Network for Pancreatic Organ Donors with Diabetes (nPOD), a collaborative Type 1 diabetes research project sponsored by the Juvenile Diabetes Research Foundation (JDRF). We obtained human islets through the integrated islet distribution program (IIDP). M.O.H. is the recipient of a Career Development Award of the JDRF. These studies were supported by grants 17–2012–424 and 2–2013–54 from the JDRF (M.O.H.), P01–DK026741 from the NIH/NIDDK (W.W.V) and the Clayton Medical Research Foundation, Inc. (M.O.H. and W.W.V.) The non–human primate studies at the Oregon National Primate Research Center (ONPRC) Obese Resource were funded by NIH/OD grant P51 OD011092 (K.L.G.). We first reported these findings at the Emerging Concepts and Targets in Islet Biology meeting in Keystone, CO on April 8, 2014 and the 73rd and 74th Scientific Sessions of the American Diabetes Association in Chicago, Il on June 23, 2013 and San Francisco, CA on June 16, 2014.

References

1. Lin HV, Accili D. Hormonal regulation of hepatic glucose production in health and disease. Cell Metab. 2011; 14:9–19. [PubMed: 21723500]
2. Leto D, Saltiel AR. Regulation of glucose transport by insulin: traffic control of GLUT4. Nat Rev Mol Cell Biol. 2012; 13:383–396. [PubMed: 22617471]
3. Ramnanan CJ, Edgerton DS, Kraft G, Cherrington AD. Physiologic action of glucagon on liver glucose metabolism. Diabetes Obes Metab. 2011; 13 (Suppl 1):118–125. [PubMed: 21824265]
4. Zhang Q, et al. Role of KATP channels in glucose-regulated glucagon secretion and impaired counterregulation in type 2 diabetes. Cell Metab. 2013; 18:871–882. [PubMed: 24315372]
5. Taborsky GJ Jr, Smith PH, Porte D Jr. Interaction of somatostatin with the A and B cells of the endocrine pancreas. Metabolism. 1978; 27:1299–1302. [PubMed: 210359]
6. Caicedo A. Paracrine and autocrine interactions in the human islet: more than meets the eye. Semin Cell Dev Biol. 2013; 24:11–21. [PubMed: 23022232]
7. Patel YC. Somatostatin and its receptor family. Front Neuroendocrinol. 1999; 20:157–198. [PubMed: 10433861]

8. Salehi A, Qader SS, Grapengiesser E, Hellman B. Pulses of somatostatin release are slightly delayed compared with insulin and antisynchronous to glucagon. Regul Pept. 2007; 144:43–49. [PubMed: 17628719]
9. Schuit FC, Derde MP, Pipeleers DG. Sensitivity of rat pancreatic A and B cells to somatostatin. Diabetologia. 1989; 32:207–212. [PubMed: 2568961]
10. Unger RH, Cherrington AD. Glucagonocentric restructuring of diabetes: a pathophysiologic and therapeutic makeover. J Clin Invest. 2012; 122:4–12. [PubMed: 22214853]
11. Braun M, et al. Somatostatin release, electrical activity, membrane currents and exocytosis in human pancreatic delta cells. Diabetologia. 2009; 52:1566–1578. [PubMed: 19440689]
12. Barden N, Alvarado-Urbina G, Cote JP, Dupont A. Cyclic AMP-dependent stimulation of somatostatin secretion by isolated rat islets of Langerhans. Biochem Biophys Res Commun. 1976; 71:840–844. [PubMed: 183781]
13. Ipp E, et al. Release of immunoreactive somatostatin from the pancreas in response to glucose, amino acids, pancreozymin-cholecystokinin, and tolbutamide. J Clin Invest. 1977; 60:760–765. [PubMed: 330567]
14. Schauder P, et al. Somatostatin and insulin release from isolated rat pancreatic islets stimulated by glucose. FEBS Lett. 1976; 68:225–227. [PubMed: 789115]
15. Patton GS, et al. Pancreatic immunoreactive somatostatin release. Proc Natl Acad Sci USA. 1977; 74:2140–2143. [PubMed: 325567]
16. Hauge-Evans AC, et al. Somatostatin secreted by islet delta-cells fulfills multiple roles as a paracrine regulator of islet function. Diabetes. 2009; 58:403–411. [PubMed: 18984743]
17. Gopel SO, Kanno T, Barg S, Rorsman P. Patch-clamp characterisation of somatostatin-secreting -cells in intact mouse pancreatic islets. J Physiol. 2000; 528:497–507. [PubMed: 11060127]
18. Vieira E, Salehi A, Gylfe E. Glucose inhibits glucagon secretion by a direct effect on mouse pancreatic alpha cells. Diabetologia. 2007; 50:370–379. [PubMed: 17136393]
19. Li C, et al. Urocortin III is expressed in pancreatic beta-cells and stimulates insulin and glucagon secretion. Endocrinology. 2003; 144:3216–3224. [PubMed: 12810578]
20. van der Meulen T, et al. Urocortin 3 marks mature human primary and embryonic stem cell-derived pancreatic alpha and beta cells. PLoS One. 2012; 7:e52181. [PubMed: 23251699]
21. Benner C, et al. The transcriptional landscape of mouse beta cells compared to human beta cells reveals notable species differences in long non-coding RNA and protein-coding gene expression. BMC Genomics. 2014; 15:620. [PubMed: 25051960]
22. Huising MO, Vale WW. CRF and Urocortins: binding proteins and receptors. Encyclopedia of Neuroscience. 2008
23. Hsu SY, Hsueh AJ. Human stresscopin and stresscopin-related peptide are selective ligands for the type 2 corticotropin-releasing hormone receptor. Nat Med. 2001; 7:605–611. [PubMed: 11329063]
24. Lewis K, et al. Identification of urocortin III, an additional member of the corticotropin-releasing factor (CRF) family with high affinity for the CRF2 receptor. Proc Natl Acad Sci USA. 2001; 98:7570–7575. [PubMed: 11416224]
25. van der Meulen T, Huising MO. Maturation of Stem Cell-Derived Beta cells Guided by the Expression of Urocortin 3. Rev Diabet Stud. 2014; 11:115–132. [PubMed: 25148370]
26. Blum B, et al. Functional beta-cell maturation is marked by an increased glucose threshold and by expression of urocortin 3. Nat Biotechnol. 2012; 30:261–264. [PubMed: 22371083]
27. Li C, Chen P, Vaughan J, Lee KF, Vale W. Urocortin 3 regulates glucose-stimulated insulin secretion and energy homeostasis. Proc Natl Acad Sci USA. 2007; 104:4206–4211. [PubMed: 17360501]
28. Huising MO, et al. Glucocorticoids differentially regulate the expression of CRFR1 and CRFR2alpha in MIN6 insulinoma cells and rodent islets. Endocrinology. 2011; 152:138–150. [PubMed: 21106875]
29. Zhang J, McKenna LB, Bogue CW, Kaestner KH. The diabetes gene Hhex maintains delta-cell differentiation and islet function. Genes Dev. 2014; 28:829–834. [PubMed: 24736842]
30. Artner I, et al. MafA and MafB regulate genes critical to beta-cells in a unique temporal manner. Diabetes. 2010; 59:2530–2539. [PubMed: 20627934]

31. Bale TL, et al. Mice deficient for corticotropin-releasing hormone receptor-2 display anxiety-like behaviour and are hypersensitive to stress. Nat Genet. 2000; 24:410–414. [PubMed: 10742108]
32. Rivier J, et al. Potent and long-acting corticotropin releasing factor (CRF) receptor 2 selective peptide competitive antagonists. J Med Chem. 2002; 45:4737–4747. [PubMed: 12361401]
33. Rorsman P, Braun M. Regulation of insulin secretion in human pancreatic islets. Annu Rev Physiol. 2013; 75:155–179. [PubMed: 22974438]
34. Rozzo A, Meneghel-Rozzo T, Delakorda SL, Yang SB, Rupnik M. Exocytosis of insulin: in vivo maturation of mouse endocrine pancreas. Ann NY Acad Sci. 2009; 1152:53–62. [PubMed: 19161376]
35. Nygaard EB, Moller CL, Kievit P, Grove KL, Andersen B. Increased fibroblast growth factor 21 expression in high-fat diet-sensitive non-human primates (Macaca mulatta). Int J Obes (Lond). 2014; 38:183–191. [PubMed: 23736354]
36. Yang YH, et al. Paracrine signalling loops in adult human and mouse pancreatic islets: netrins modulate beta cell apoptosis signalling via dependence receptors. Diabetologia. 2011; 54:828–842. [PubMed: 21212933]
37. Rodriguez-Diaz R, et al. Alpha cells secrete acetylcholine as a non-neuronal paracrine signal priming beta cell function in humans. Nat Med. 2011; 17:888–892. [PubMed: 21685896]
38. Xu E, et al. Intra-islet insulin suppresses glucagon release via GABA-GABAA receptor system. Cell Metab. 2006; 3:47–58. [PubMed: 16399504]
39. Yang YH, Manning Fox JE, Zhang KL, MacDonald PE, Johnson JD. Intraislet SLIT-ROBO signaling is required for beta-cell survival and potentiates insulin secretion. Proc Natl Acad Sci USA. 2013; 110:16480–16485. [PubMed: 24065825]
40. Ohtani O, Ushiki T, Kanazawa H, Fujita T. Microcirculation of the pancreas in the rat and rabbit with special reference to the insulo-acinar portal system and emissary vein of the islet. Arch Histol Jpn. 1986; 49:45–60. [PubMed: 3524504]
41. Liu YM, Guth PH, Kaneko K, Livingston EH, Brunicardi FC. Dynamic in vivo observation of rat islet microcirculation. Pancreas. 1993; 8:15–21. [PubMed: 8419903]
42. Murakami T, et al. The insulo-acinar portal and insulo-venous drainage systems in the pancreas of the mouse, dog, monkey and certain other animals: a scanning electron microscopic study of corrosion casts. Arch Histol Cytol. 1993; 56:127–147. [PubMed: 8373657]
43. Bonner-Weir S, Orci L. New perspectives on the microvasculature of the islets of Langerhans in the rat. Diabetes. 1982; 31:883–889. [PubMed: 6759221]
44. Stagner JI, Samols E, Bonner-Weir S. beta----alpha----delta pancreatic islet cellular perfusion in dogs. Diabetes. 1988; 37:1715–1721. [PubMed: 2903837]
45. Samols E, Stagner JI. Islet somatostatin--microvascular, paracrine, and pulsatile regulation. Metabolism. 1990; 39:55–60. [PubMed: 1976222]
46. Nyman LR, et al. Real-time, multidimensional in vivo imaging used to investigate blood flow in mouse pancreatic islets. J Clin Invest. 2008; 118:3790–3797. [PubMed: 18846254]
47. Benninger RK, Zhang M, Head WS, Satin LS, Piston DW. Gap junction coupling and calcium waves in the pancreatic islet. Biophys J. 2008; 95:5048–5061. [PubMed: 18805925]
48. Ravier MA, et al. Loss of connexin36 channels alters beta-cell coupling, islet synchronization of glucose-induced Ca2+ and insulin oscillations, and basal insulin release. Diabetes. 2005; 54:1798–1807. [PubMed: 15919802]
49. Head WS, et al. Connexin-36 gap junctions regulate in vivo first- and second-phase insulin secretion dynamics and glucose tolerance in the conscious mouse. Diabetes. 2012; 61:1700–1707. [PubMed: 22511206]
50. Jorgensen MC, et al. An illustrated review of early pancreas development in the mouse. Endocr Rev. 2007; 28:685–705. [PubMed: 17881611]
51. Herrera PL, et al. Embryogenesis of the murine endocrine pancreas; early expression of pancreatic polypeptide gene. Development. 1991; 113:1257–1265. [PubMed: 1811941]
52. Gromada J, Franklin I, Wollheim CB. Alpha-cells of the endocrine pancreas: 35 years of research but the enigma remains. Endocr Rev. 2007; 28:84–116. [PubMed: 17261637]

53. Unger RH, Orci L. Paracrinology of islets and the paracrinopathy of diabetes. Proc Natl Acad Sci USA. 2010; 107:16009–16012. [PubMed: 20798346]
54. Huising MO, et al. CRFR1 is expressed on pancreatic beta cells, promotes beta cell proliferation, and potentiates insulin secretion in a glucose-dependent manner. Proc Natl Acad Sci USA. 2010; 107:912–917. [PubMed: 20080775]
55. Consortium EP. An integrated encyclopedia of DNA elements in the human genome. Nature. 2012; 489:57–74. [PubMed: 22955616]
56. Huising MO, et al. Residues of corticotropin releasing factor-binding protein (CRF-BP) that selectively abrogate binding to CRF but not to urocortin 1. J Biol Chem. 2008
57. Asfari M, et al. Establishment of 2-mercaptoethanol-dependent differentiated insulin-secreting cell lines. Endocrinology. 1992; 130:167–178. [PubMed: 1370150]
58. Taniguchi H, et al. A resource of Cre driver lines for genetic targeting of GABAergic neurons in cerebral cortex. Neuron. 2011; 71:995–1013. [PubMed: 21943598]
59. Herrera PL. Adult insulin- and glucagon-producing cells differentiate from two independent cell lineages. Development. 2000; 127:2317–2322. [PubMed: 10804174]
60. Srinivas S, et al. Cre reporter strains produced by targeted insertion of EYFP and ECFP into the ROSA26 locus. BMC Dev Biol. 2001; 1:4. [PubMed: 11299042]
61. Reubi JC, et al. SST3-selective potent peptidic somatostatin receptor antagonists. Proc Natl Acad Sci USA. 2000; 97:13973–13978. [PubMed: 11095748]
62. Cescato R, et al. Design and in vitro characterization of highly sst2-selective somatostatin antagonists suitable for radiotargeting. J Med Chem. 2008; 51:4030–4037. [PubMed: 18543899]
63. Dobin A, et al. STAR: ultrafast universal RNA-seq aligner. Bioinformatics. 2013; 29:15–21. [PubMed: 23104886]
64. Quinlan AR, Hall IM. BEDTools: a flexible suite of utilities for comparing genomic features. Bioinformatics. 2010; 26:841–842. [PubMed: 20110278]
65. Anders S, Huber W. Differential expression analysis for sequence count data. Genome Biol. 2010; 11:R106. [PubMed: 20979621]
66. Heinz S, et al. Simple combinations of lineage-determining transcription factors prime cis-regulatory elements required for macrophage and B cell identities. Mol Cell. 2010; 38:576–589. [PubMed: 20513432]
67. Brazeau P, et al. Hypothalamic polypeptide that inhibits the secretion of immunoreactive pituitary growth hormone. Science. 1973; 179:77–79. [PubMed: 4682131]
68. Vale W, Rivier J, Ling N, Brown M. Biologic and immunologic activities and applications of somatostatin analogs. Metabolism. 1978; 27:1391–1401. [PubMed: 210361]
69. Vaughan JM, et al. Detection and purification of inhibin using antisera generated against synthetic peptide fragments. Methods Enzymol. 1989; 168:588–617. [PubMed: 2725313]
70. Padmanabhan K, Eddy WF, Crowley JC. A novel algorithm for optimal image thresholding of biological data. J Neurosci Methods. 2010; 193:380–384. [PubMed: 20817033]

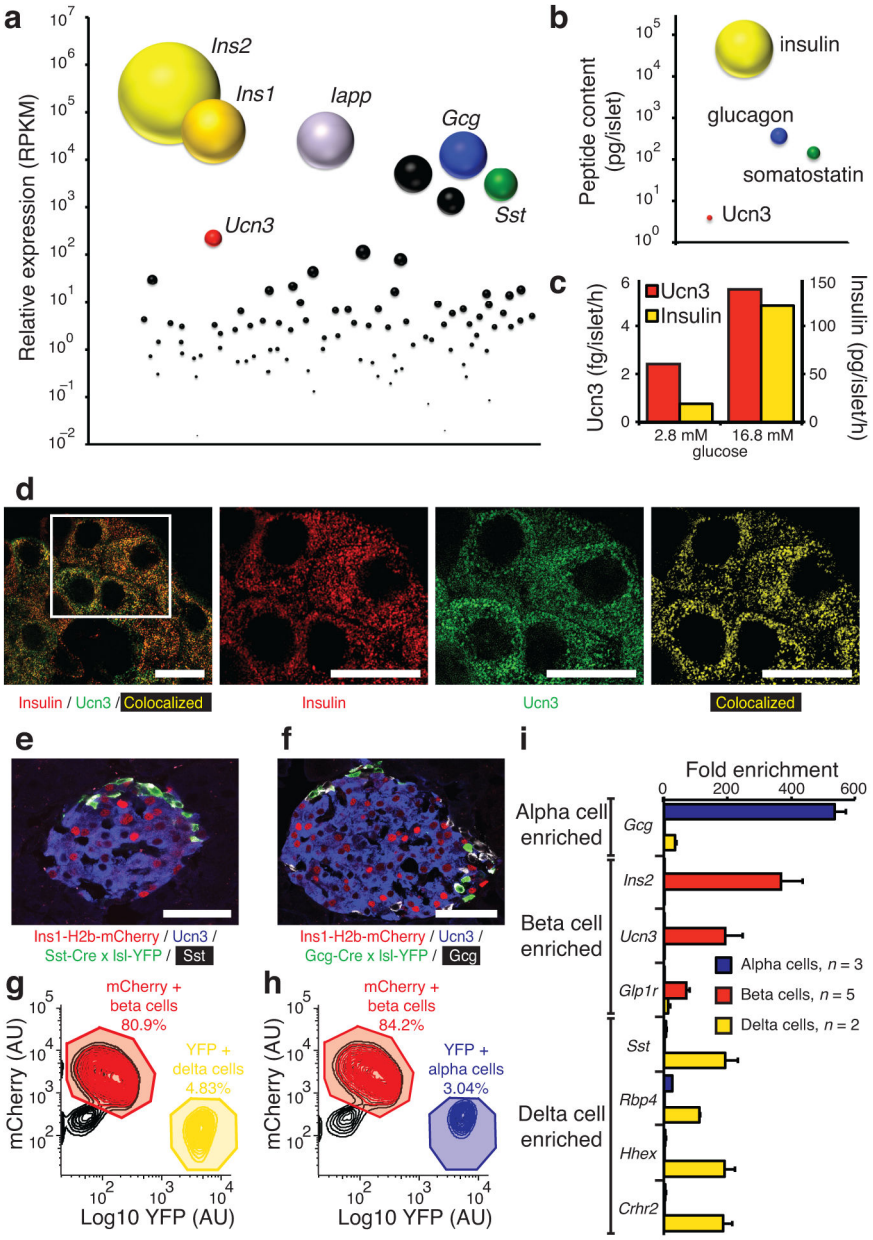

Figure 1.

Ucn3 is a paracrine factor expressed by mouse beta cells. (**a**) Quantification of the expression of *Ucn3* relative to all genes that encode secreted factors in wild–type mouse islets. (**b**) Comparison of islet Ucn3 peptide content to other islet hormones. (**c**) Comparison of Ucn3 and insulin secretion from mouse islets in response to glucose (1000 islets/well; Ucn3 Mw, 4174; insulin Mw, 5785). (**d**) Ucn3 and insulin colocalize in secretory granules of mouse beta cells by Super Resolution Structured Illumination Microscopy with thresholded Manders' coefficients for insulin and Ucn3 of 62.7% and 59.6%, respectively. Images of a *mIns1*–H2b–mCherry reporter line crossed to either a *Sst*–Cre (**e**) or *Gcg*–Cre (**f**) allele and a floxed YFP reporter. FACS purification of mCherry^{+} beta cells and delta (**g**) or alpha (**h**) cells. (**i**) Gene expression by quantitative PCR of *Crhr2* and a panel of

established alpha, beta and delta cell markers. AU = arbitrary units. Scale bars, 10 μm (**d**) and 50 μm (**e**, **f**). All values are mean ± s.e.m.

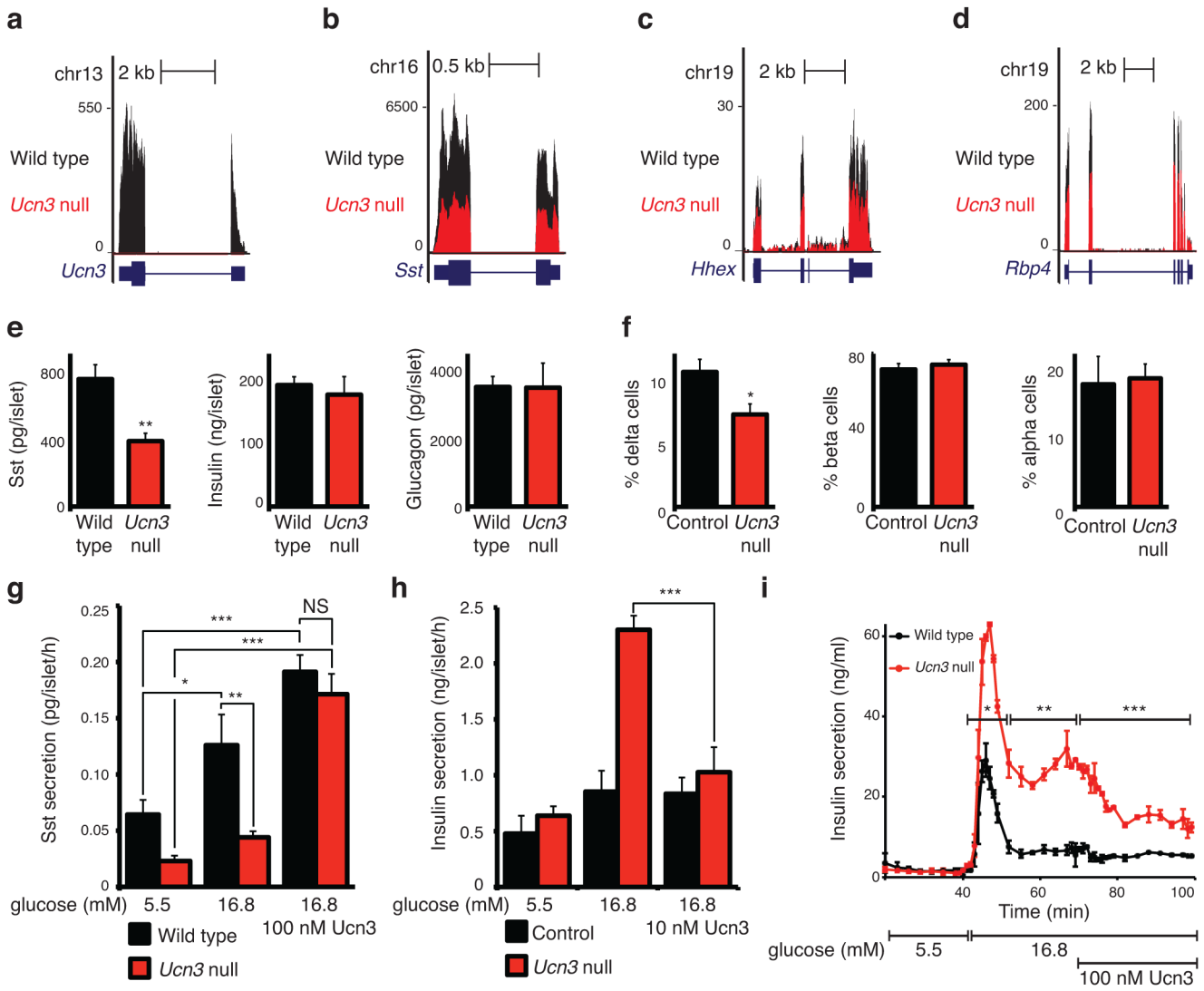

Figure 2.

Ucn3–null islets are deficient in delta cell number and somatostatin secretion. Transcriptome analysis of *Ucn3*–null islets compared to wild–type littermates for *Ucn3* (**a**) *Sst* (**b**), *Hhex* (**c**), and *Rbp4* (**d**) ($n = 3$), data normalized to 1×10^7 reads. (**e**) Somatostatin, insulin and glucagon content of *Ucn3*–null and control islets ($n = 4$). (**f**) Relative delta, beta and alpha cell number of *Ucn3* null and control islets ($n = 3$ control/4 *Ucn3* null, 5–7 islets/animal). (**g**) Somatostatin secretion from *Ucn3*–null islets compared to control ($n = 4$, 95 islets/well, asterisks indicate significance with the 5.5 mM glucose group for the same genotype, unless indicated otherwise). Insulin secretion from *Ucn3*–null islets compared to control in static incubation (**h**) ($n = 4$, 7 islets/well) and in islet perfusion (**i**) ($n = 2$, 150 islets per chamber, representative of 2 experiments). Significance determined by Student's t–test (**e**, **f**), two–way ANOVA for treatment and genotype, followed by Holm–Sidak's multiple comparison test (**g**, **h**), or two–way ANOVA for genotype and its interaction with time for each block (**i**); *P* values for genotype are given (**i**). All values are mean ± s.e.m., $*P < 0.05$, $**P < 0.01$, $***P < 0.001$.

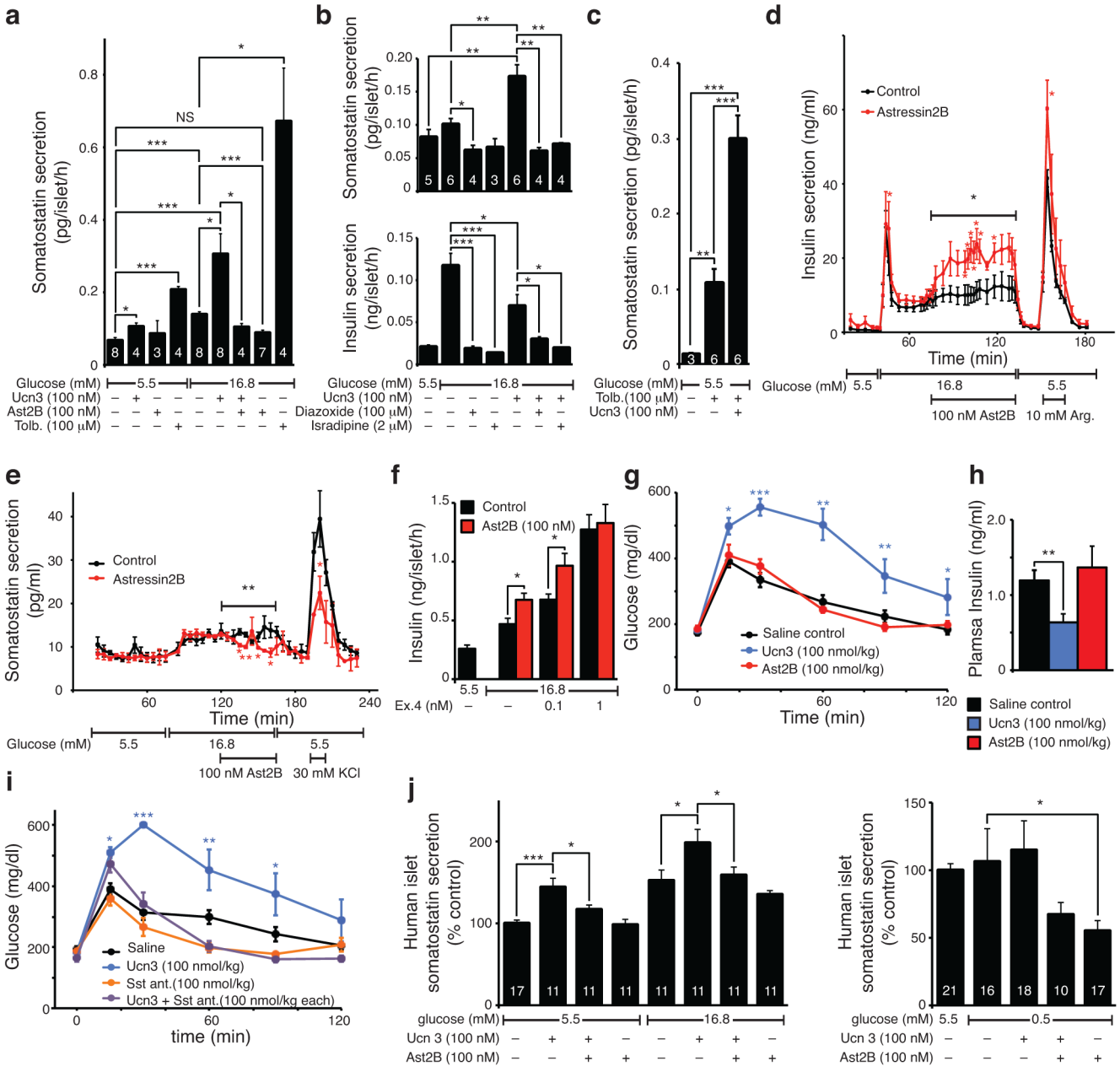

Figure 3.

Endogenous Ucn3 promotes somatostatin–mediated negative feedback. (**a**) Somatostatin secretion from wild type mouse islets in response to Ucn3 or its antagonist Ast2B (*n* indicated in each bar, 100 islets/well). Interactions between Ucn3 and diazoxide or isradipine on somatostatin (**b**, top, *n* indicated in each bar, 50 or 100 islets/well) or insulin secretion (**b**, bottom, *n* = 7, 12 islets/well). (**c**) Ucn3 amplifies somatostatin secretion induced by tolbutamide (*n* indicated in each bar, 80 or 50 islets/well). Inhibition of endogenous Ucn3 by Ast2B acutely de–represses insulin secretion (**d**) via reduced somatostatin release (**e**) (*n* = 3, 150 (**d**) or 270 (**e**) islets/chamber). (**f**) Ast2B enhances exendin4 (Ex4) –induced insulin secretion (*n* = 6, 12 islets/well). Ucn3 impairs glucose

tolerance (**g**) and suppresses glucose–stimulated plasma insulin (**h**) *in vivo*, while Ast2B has no effect ($n = 7$ for saline and Ucn3 groups, $n = 6$ for Ast2B). (**i**) Ucn3–mediated glucose intolerance is prevented by somatostatin antagonists ($n = 5$). (**j**) Effects of Ucn3 and Ast2B on insulin secretion from human islets (*n* indicated in each bar, 50 islets/well; normalized secretion across 2 (left) or 3 (right individual donors). Significance determined by one–way ANOVA followed by Student's t–test with Welch's correction for unequal variance as necessary (**a**, **b**, **c**, **f**, **h**, **j**), two–way ANOVA for the interaction of treatment and time for each block, followed by the comparison of individual time points by Student's t–test (**d**, **e**) or two–way ANOVA for treatment and its interaction with time, followed by Holm–Sidak's multiple comparison test (**g**, **i**). NS = not significant. All values are mean ± s.e.m., $*P < 0.05$, $**P < 0.01$, $***P < 0.001$.

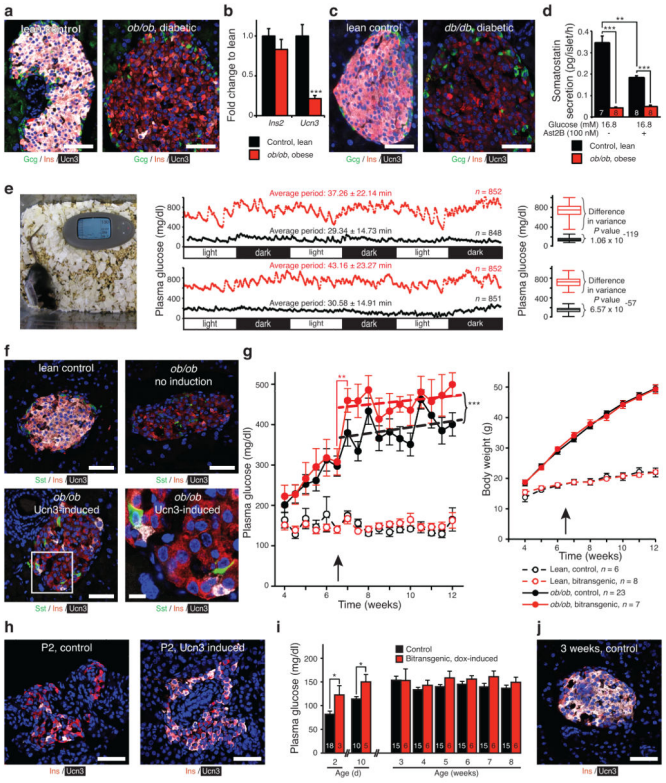

Figure 4.

Ucn3 marks mature beta cells and aggravates hyperglycemia. Ucn3 immunoreactivity (**a**) and gene expression (**b**) (n = 9 controls, n = 8 *ob/ob*) in islets from *ob/ob* and *db/db* mice (**c**). (**d**) Somatostatin release from *ob/ob* islets compared to lean controls in response to Ast2B. (**e**) Loss of Ucn3 correlates with increased glycemic volatility and extended period length in *ob/ob* animals compared to lean controls, n reflects the number of data points, P values reflect differences in variance between animals, see Supplementary Table 2. (**f**) Doxycycline–inducible Ucn3 overexpressing mice (Supplementary Fig. 5) crossed on the *ob/ob* background facilitate the restoration of Ucn3 expression by beta cells. (**g**) Effect of Ucn3 induction on plasma glucose and body weight in doxycycline-inducible Ucn3 overexpressing mice. (**h**, **i**, **j**) Effect of Ucn3 induction on plasma glucose before and after endogenous Ucn3 is expressed in all beta cells. Scale bars, 50 μm in all panels except the detail in **f**, lower right (10 μm). Significance determined by Student's t–test (**b**, **i**) or by one–way ANOVA followed by Student's t–test with Welch's correction as necessary (**d**) or by linear regression between groups before and after induction (**g**), and Student's t–test to compare the glucose values immediately before and after induction. Significance of Ucn3 induction in (**i**) determined by Student's t–test for P2 and P10 groups and by two–way ANOVA for treatment and time for older ages. Values are mean ± s.d. in (**e**) and mean ± s.e.m. in all other panels, *P < 0.05, **P < 0.01, ***P < 0.001.

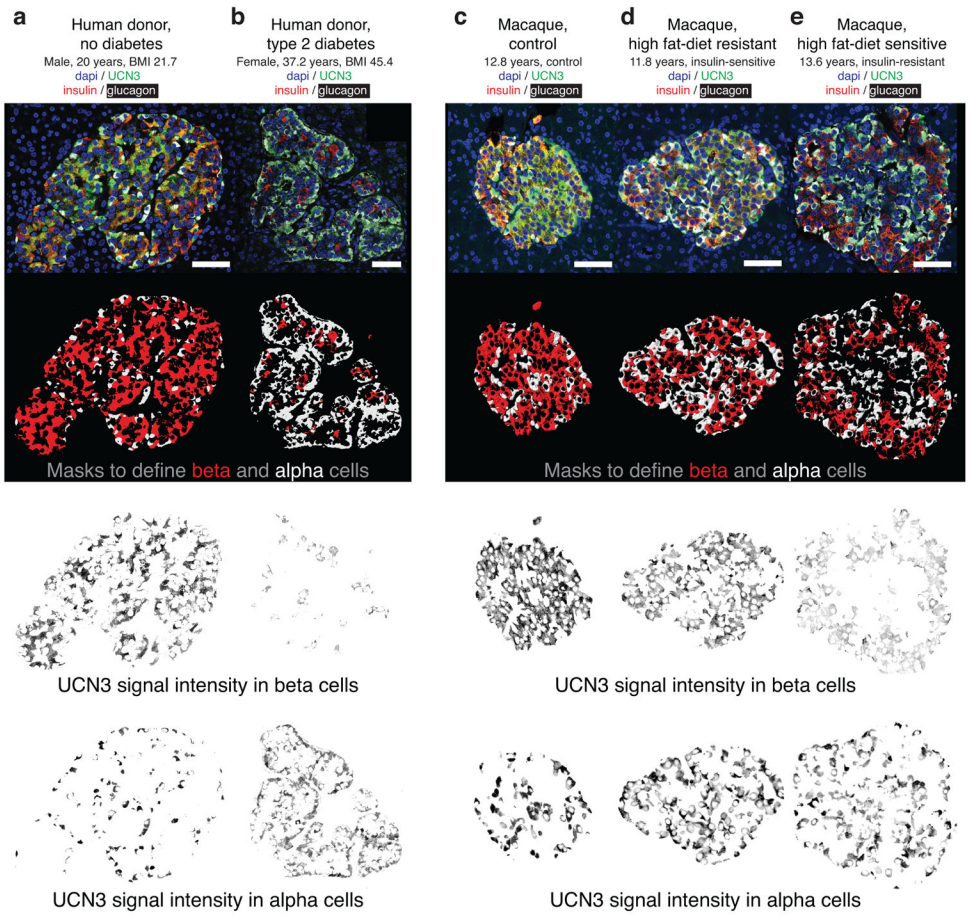

Figure 5.

UCN3 is lost from beta cells of Type 2 diabetic humans and pre–diabetic macaques. UCN3 in islets of a 20–year old non–diabetic donor with a healthy BMI (**a**), and in a 37–year old morbidly obese Type 2 diabetic donor (**b**). We applied masks based on insulin (red) and glucagon (white) to isolate UCN3 staining in beta and alpha cells. Data for 16 additional human donors with and without diagnosed Type 2 diabetes are presented in Supplementary Fig. 7 and support these observations. UCN3 staining in macaques on control diet (**c**) and on a high–fat diet classified as ‘diet–resistant’ (**d**) and ‘diet–sensitive’ (**e**). Similar data for 14 additional macaques across these cohorts are presented in Supplementary Fig. 8 and support these observations. Scale bars, 50 μm.

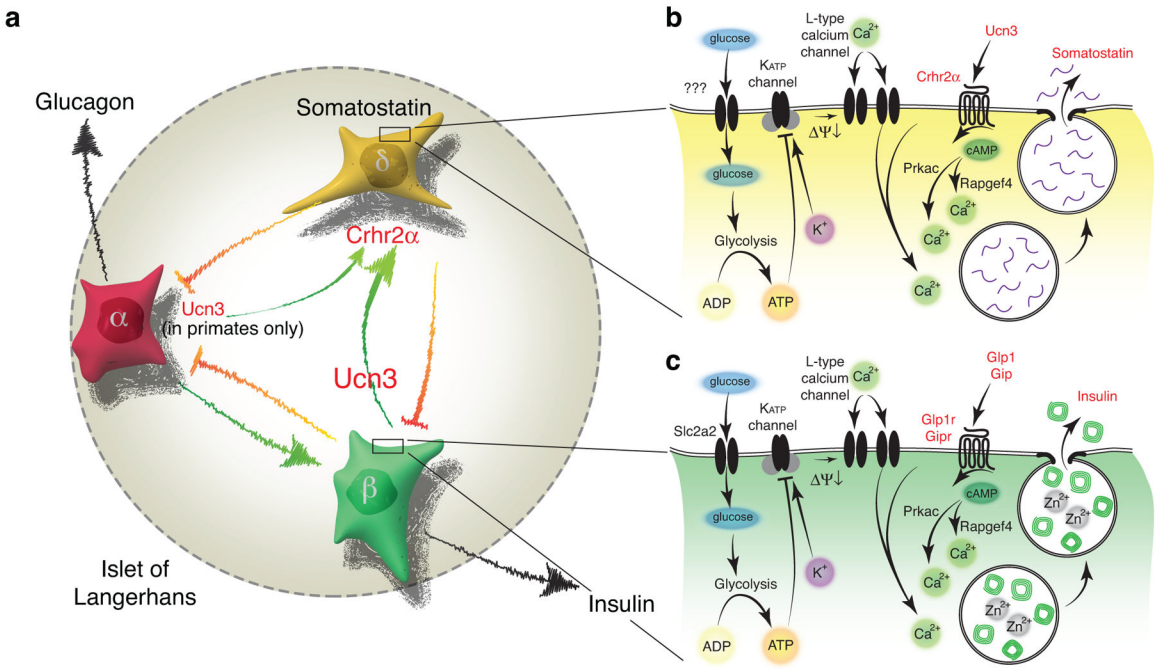

Figure 6.

Ucn3 promotes somatostatin secretion from delta cells in an incretin–like fashion. (**a**) Insulin and other factors secreted by the beta cell are generally considered inhibitory to glucagon secretion, while alpha cell hormones, paradoxically, stimulate insulin release. Ucn3 from beta and human alpha cells is a paracrine signal that stimulates somatostatin via Crhr2α receptors expressed by delta cells. This drives negative feedback and attenuates insulin and glucagon secretion once glucose homeostasis is restored. (**b**) Dependence of Ucn3–stimulated somatostatin secretion on K_{ATP} and L–type voltage–gated calcium channels suggests that delta cell–autonomous stimulus secretion coupling is required to trigger somatostatin release and is potentiated by Ucn3 acting through Crhr2α expressed by delta cells. (**c**) While the term ‘incretin’ is *sensu strictu* reserved for hormones of gastro–intestinal origins that potentiate glucose–stimulated insulin secretion, the actions of Ucn3 on the delta cell mechanistically resemble the actions of incretins on the beta cell as both cells respond to a class B GPCR peptide ligand to potentiate exocytosis under elevated ambient glucose conditions. ΔΨ↓, membrane depolarization.